Published January 28, 2010 as 10.3174/ajnr.A1971

PATIENT SAFETY

Dose Exposure of Patients Undergoing Comprehensive Stroke Imaging by Multidetector-Row CT: Comparison of 320-Detector Row and 64-Detector Row CT Scanners

S. Diekmann
E. Siebert
R. Juran
M. Roll
W. Deeg
H.-C. Bauknecht
F. Diekmann
R. Klingebiel
G. Bohner

BACKGROUND AND PURPOSE: Recently introduced 320-detector row CT enables whole brain perfusion imaging compared to a limited scanning area in 64-detector row CT. Our aim was to evaluate patient radiation exposure in comprehensive stroke imaging by using multidetector row CT consisting of standard CT of the head, CTA of cerebral and cervical vessels, and CTP.

MATERIAL AND METHODS: Organ doses were measured by using LiF-TLDs located at several organ sites in an Alderson-Rando phantom. Effective doses were derived from these measurements. Stroke protocols including noncontrast head CT, CTA of cerebral and cervical vessels, and CTP were performed on 320- and 64-detector row scanners.

RESULTS: Measured effective doses for the different scanning protocols ranged between 1.61 and 4.56 mSv, resulting in an effective dose for complete stroke imaging of 7.52/7.54 mSv (m/f) for 64-detector row CT and 10.56/10.6 mSv (m/f) for 320-detector row CT. The highest organ doses within the area of the primary beam were measured in the skin (92 mGy) and cerebral hemispheres (69.91 mGy). Use of an eye-protection device resulted in a 54% decrease of the lens dose measured for the combo protocol for whole-brain perfusion with the 320-detector row CT scanner.

CONCLUSIONS: Phantom measurements indicate that comprehensive stroke imaging with multidetector row CT may result in effective radiation doses from 7.52 mSv (64-detector row CT) to 10.6 mSv (320-detector row CT). The technique of 320-detector row CT offers additional information on the time course of vascular enhancement and whole-brain perfusion. Physicians should weigh the potential of the new technique against the higher radiation dose that is needed. Critical doses that would cause organ damage were not reached.

ABBREVIATIONS: CCT = cerebral CT; CTA = CT angiography; CTDI = CT Dose Index; CTP = CT perfusion; ICA = internal carotid artery; ICRP = International Commission on Radiological Protection; LiF = lithium-fluoride; mAs_{eff} = effective milliampere-second; m/f = male/female; PMMA = polymethylmethacrylate; TLD = thermoluminescent dosimeter; W (T) = weighting factor

CTP in conventionally used multidetector row CT scanners used to be hampered by perfusion data only being obtained for a small scanning area compared with MR imaging.[1,2] The scanning-area width is determined by the detector width and ranges from approximately 32 to 40 mm for 64-detector row CT scanners from different manufacturers. To overcome this problem, Roberts et al[3] presented in 2001 the so-called toggling technique for scanning of a larger region by acquisition of alternating scans in 2 different toggling-table positions after administration of a single bolus of contrast medium. Recently introduced CT with 320 detector rows now enables perfusion imaging of the entire neurocranium. Regarding CTA, the increased detector width enables dynamic scanning of the entire intracranial vasculature (4D CTA). The cervical vessels are imaged by acquisition of an additional spiral CT scan, analogous to 64-detector row CT. Data on the radiation exposure of 320-detector row CT examinations are still limited. The aim of the present study, therefore, was to compare the radiation exposure of stroke imaging performed on 320-detector row CT scanners with that of 64-detector row CT and to discuss the radiation exposure in relation to the diagnostic benefit expected from dynamic scan data and whole-brain perfusion imaging.

For measurement of the radiation dose in CT, the CTDI is used. CDTI 100 is determined by using a 100-mm pencil ion chamber with a cylindrical PMMA dosimetry phantom. This definition of CTDI 100 is adequate for CT scanners with a detector width of $\leq$10 cm but needs to be modified for application to multisection CT scanners with greater detector widths.[4-6] The radiation dose of CT with a scanning length $>$10 cm is, therefore, given as CTDI "extended." To ensure accurate assessment of patient doses by using standard dosimetry methods, Mori et al[7-9] developed a conversion factor for CT dosimetry on a 256-section CT scanner. A recently published article by Geleijns et al[6] emphasizes the need for development of new metrics in CT dosimetry for application in wide conebeam CT. CTDI values that are provided by the

Received September 1, 2009; accepted after revision October 25.

From the Department of Neuroradiology (S.D., E.S., R.J., H.-C.B., R.K., G.B.), Charité Centrum 6, Charité Campus Mitte, Berlin, Germany; TFH Berlin (M.R., W.D.), Beuth Hochschule für Technik, Fachbereich 2, Fachgruppe Physik, Labor für Röntgentechnik, Berlin, Germany; and Department of Radiology (F.D.), Charité Centrum 6, Charité Campus Virchow, Berlin, Germany.

Paper previously presented as a poster at: Annual Meeting of the American Society of Neuroradiology, May 16–21, 2009; Vancouver, British Columbia, Canada.

Please address correspondence to Susanne Diekmann, MD, Department of Neuroradiology, Charité Centrum 6, Charité–University Medicine Berlin, 10117 Berlin, Germany; e-mail: susanne.diekmann@charite.de

DOI 10.3174/ajnr.A1971

Table 1: Doses measured for all protocols on 64-row scanner (Toshiba Aquilion 64)

		Noncontrast Head CT		Perfusion		CTA	
Organ	W (T)	Dose (mGy)	Weighted Dose (mSv)	Dose (mGy)	Weighted Dose (mSv)	Dose (mGy)	Weighted Dose (mSv)
Hemispheres	0.01	33.31	0.33	66.22	0.66	24.34	0.24
Skin (within scan area)		33.17		75.41		26.27	
Skin (total)	0.01	17.43	0.17	37.9	0.38	13.87	0.14
Eye lenses		41.69		6.74		14.86	
Pituitary gland		33.7		14.26		20.07	
Bone marrow (scan area)		8.4		4.1		22.05	
Bone marrow (total)	0.12	4.6	0.56	2.36	0.28	11.88	1.43
Thyroid gland	0.04	1.49	0.06	1.04	0.04	39.17	1.57
Lung	0.12	0.8	0.1	0.48	0.06	2.99	0.36
Esophagus	0.04	0.36	0.01	0.55	0.02	2.78	0.11
Breast	0.12	1.69	0.2	0.39	0.05	1.47	0.18
Liver	0.05	0.37	0.02	0.28	0.01	0.94	0.05
Stomach	0.12	0.53	0.06	0.44	0.05	0.92	0.11
Ovaries	0.08	0.28	0.02	0.33	0.03	0.35	0.03
Lower colon	0.12	0.74	0.09	0.28	0.03	0.24	0.03
Bladder	0.04	0.73	0.03	0.34	0.01	0.57	0.02
Testes	0.08	0.31	0.02	0.27	0.02	0.28	0.02
Effective dose (women)			1.65		1.62		4.27
Effective dose (men)			1.65		1.61		4.26

scanner after each protocol, therefore, vary according to the detector width of the scanner. To overcome problems with different CTDI definitions for comparison of dose exposure by using CT scanners with different detector widths, we used TLDs and phantom-based dose measurement to achieve accurate and reproducible results.

Materials and Methods

Phantoms and Dose Measurement

The experiments were performed by using an anthropomorphic Alderson-Rando phantom (Phantom Laboratory, Salem, New York) and an LiF-TLD (TLD 100, Harshaw, Cleveland, Ohio), 6 × 1 mm, for dose measurement. By using a BV-25 (Philips Medical Systems, Best, the Netherlands), we calibrated the TLDs according to the tube potential: 1) 80 kV, 4-mm Al filtering (inbuilt and additional filters), dose of approximately 4 mGy; 2) 100 kV, 4-mm Al filtering, dose of approximately 6 mGy. Group 1 TLDs were used for combined scans (so-called "combo" scans, see "Protocols" for details) (80 kV); those of group 2 were used for all other protocols (120 kV). The TLDs were read out after heating and annealing (TLDO oven; PTW, Freiburg, Germany) in a Harshaw reader (TLD3500, Harshaw) within 24 hours of measurement.

A total of 27 TLDs were placed in defined sites for each protocol. The sites included relevant organs in the scanning area (brain, eye lenses, pituitary gland, thyroid, skin) and sensitive organs outside the scanning area (spinal cord, ovaries, testes). Two TLDs were placed per site in these organs. The mean values measured for each site are summarized in Tables 1 and 2 .

The skin dose was measured in the frontal, temporal, and occipital regions. Temporal skin dose dosimeters were placed within the scanning area of 64-detector row CT (Figs 1 and 2*E*). The spinal cord dose was measured by using TLDs placed at the levels of C1 and C5 (within the scanning area) and T3 and T8 (outside the scanning area). Following the ICRP 103 recommendations, we placed additional TLDs in the relevant organs and tissues for calculation of the effective dose (1 TLD per site).[10] Because the primary aim of our experiment was to determine organ doses in the head region for comparison of 64-detector row and 320-detector row CT and because the dose drops sharply outside the scanning area, we did not measure doses at all remaining sites of the body according to ICRP 103. The sites of TLDs are shown in Fig 1. Because the measurement sites in the simulated organs were determined by the bores in the phantom, accurate placement in smaller organs was not possible. Therefore, 2 TLDs were placed in the pituitary gland, 1 frontally and 1 posteriorly, adjacent to the sellar fossa. The TLD for measuring the breast dose was attached to the phantom surface; an additional breast phantom was not used. Superficially attached TLDs were also used for measuring the doses to the eye lenses and the testes.

The dose reduction was accomplished with use of an eye lens shield made of an alloy mainly consisting of bismuth, antimony, gadolinium, and tungsten[25] (CT-Eye Protex, Somatex Medical Technologies, Teltow, Germany) and was investigated by using a film dosimetry technique (Kodak X-Omat V, Eastman Kodak Company, Rochester, New York) with a cylindrical PMMA head phantom (160 mm in diameter). Film dosimetry was used in addition to the previous measurement with thermoluminescent dosimetry because of its superior spatial resolution.[11] Results of previous studies[12-14] indicate that the accuracy of film dosimetry is approximately ±15% compared with that of thermoluminescent dosimetry. The lens dose was measured for the combo protocol on the 320-detector row CT scanner without and with both eye lens shields, which were used for the measurements with both the 64- and 320-detector row scanners. The verification films were analyzed after calibration (Diados, PTW) by using optical attenuation (calibrated film verification method).

Protocols

Radiation dose measurements were performed on a 64-detector row CT scanner (Aquilion 64; Toshiba Medical Systems, Tokyo, Japan) and on a 320-detector row scanner (Aquilion ONE, Toshiba Medical Systems) by using standardized protocols for comprehensive stroke imaging,[15] which include noncontrast head CT scans, perfusion imaging, and scanning of the cervicocranial vessels starting at the aortic

Table 2: Doses measured for all protocols on a 320-row scanner (Toshiba Aquilion ONE)

		Noncontrast Head CT Volume		Noncontrast Head CT Incremental		CTP + CTA (Intracranial)		CTA (Neck)	
Organ	W (T)	Dose (mGy)	Weighted Dose (mSv)	Dose (mGy)	Weighted Dose (mSv)	Dose (mGy)	Weighted Dose (mSv)	Dose (mGy)	Weighted Dose (mSv)
Hemispheres	0.01	31.42	0.31	41.91	0.42	69.91	0.7	3.34	0.03
Skin (scan area)		36.86		42.34		92		3.84	
Skin (total)	0.01	19.19	0.19	21.47	0.21	46.49	0.46	3	0.03
Eye lenses		40.23		44.31		44.01		2.39	
Pituitary gland		25.24		38.93		52.69		5.3	
Bone marrow (scan area)		7.67		12.77		30.17		14.8	
Bone marrow (total)	0.12	4.2	0.5	6.97	0.84	15.81	1.9	8.57	1.03
Thyroid gland	0.04	2.54	0.1	3.39	0.14	5.37	0.21	58.6	2.3
Lung	0.12	0.78	0.09	0.4	0.05	0.61	0.07	4.36	0.5
Esophagus	0.04	0.5	0.02	0.63	0.03	0.46	0.02	3.51	0.14
Breast	0.12	1.52	0.18	0.59	0.07	0.98	0.12	2.17	0.26
Liver	0.05	0.77	0.04	0.42	0.02	0.29	0.01	1.16	0.06
Stomach	0.12	0.63	0.08	0.3	0.04	0.29	0.03	1.18	0.14
Ovaries	0.08	0.48	0.04	1.01	0.08	0.42	0.03	0.36	0.03
Lower colon	0.12	0.46	0.06	0.43	0.51	0.23	0.03	0.29	0.03
Bladder	0.04	0.68	0.03	0.59	0.02	0.74	0.03	0.33	0.01
Testes	0.08	0.29	0.02	0.53	0.04	0.43	0.03	0.34	0.03
Effective dose (women)			1.64		2.43		3.61		4.56
Effective dose (men)			1.62		2.39		3.61		4.56

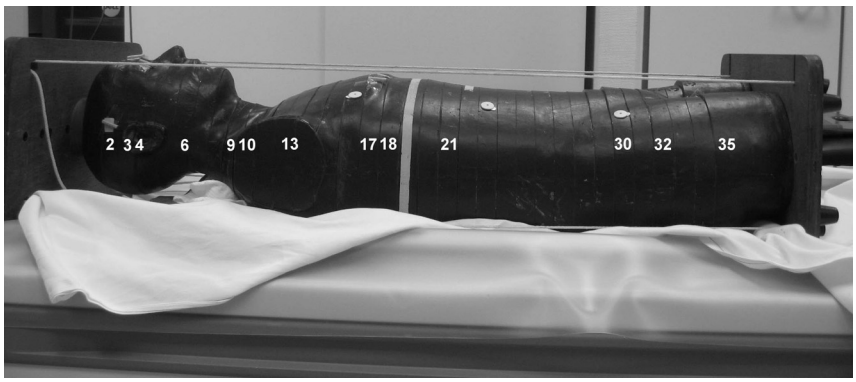

Fig 1. Alderson-Rando phantom. Numbers indicate the sections in which TLDs were placed (Table 1).

arch. For a 64-detector row scanner, the recommended protocol consists of a noncontrast incremental CCT; a CTP, which has a length of 32 mm on the scanner we used; and CTA in the helical mode extending from the origin of the cervicocranial arteries from the aortic arch to the vertex (34 cm). A slight deviation from the standardized protocol had to be made in terms of angulation because this was influenced by the shape of the phantom (see below).

The corresponding protocols for the 320-detector row CT scanner were comparable in terms of scanning technique and diagnostic information. We used both scanning modes available on the 320-detector row CT scanner for unenhanced CCT: 1) acquisition of a volume dataset during a single rotation, and 2) an incremental CT scan analogous to the protocol for 64-detector row CT. With the 320-detector row scanner, a perfusion study and dynamic angiography of the cerebral arteries and veins can be performed in 1 procedure. This so-called combo protocol was used with coverage of the entire neurocranium (14-cm scanning length). The dataset acquired with the combo protocol allows generation of both whole-brain perfusion maps and time-resolved angiograms of the cerebral arteries and veins. The examination on the 320-detector row CT scanner was supplemented by neck CTA (spiral scanning analogous to the 64-detector CT protocol), resulting in a total scanning length of the CTA protocol of 34 cm (ie, the same as for 64-detector row CT). Details of the scanning parameters are summarized in Tables 3 and 4.

Following scanogram acquisition in lateral and frontal projections, we manually prescribed the noncontrast CCT in accordance with clinical standards and aligned the gantry angulation to the supraorbitomeatal line (Fig 2). Gantry angulation was limited by the fact that the metallic stabilizers at the head end of the phantom had to lie outside the scanning area to minimize beam-hardening artifacts; therefore, parts of the orbits and eye lenses were within the scanning area. Care was taken to ensure use of identical angulations, section thicknesses, and scanning areas on both CT scanners investigated. The standard CT protocols were acquired in the sequential mode on both scans as in the routine clinical situation. On the 320-detector row CT scanner, an additional volume scan was acquired. Noncon-

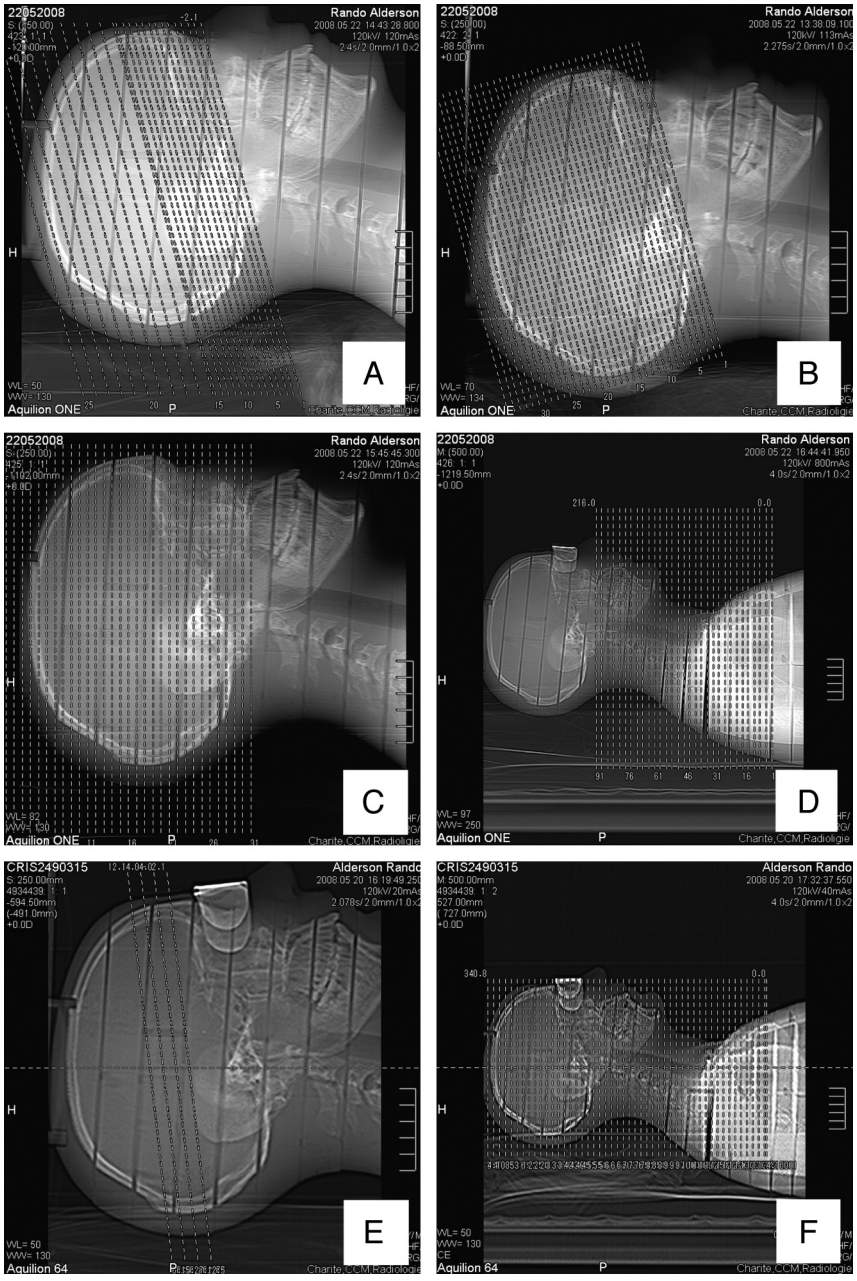

Fig 2. Scanograms of the 320-detector row CT scanner: *A*, incremental CCT; *B*, volume CCT; *C*, combo protocol; *D*, neck CT. Scanograms of the 64-detector row CT scanner: *E*, CTP; *F*, CTA (head and neck) (incremental CCT is analogous to *A*).

trast head CT was performed without lens protection because the eye lenses are outside the scanning area when standard gantry angulation is used. Gantry angulation was also used for planning CTP on the 64-detector row CT scanner with placement of the scanning area at the level of the basal ganglia. The combo protocol on the 320-detector row CT scanner (combining CTA of the intracranial vessels and CTP) with a 14-cm scanning length and covering the entire neurocranium was performed without gantry angulation. CTA on the 64-detector row scanner and cervical CTA on the 320-detector row scanner were also performed without gantry angulation.

The CTA scanning extended from the origin of the cervicocranial arteries from the aortic arch to the superior sagittal sinus (ie, from the T5 vertebra to the vertex). CTA of the cerebral vessels on the 320-detector row scanner consisted of the combo protocol and neck CTA, resulting in an identical overall scanning length of 34 cm. CTP, combo, and CTA were performed with a lens-protection device (CT-Eye Protex, Somatex Medical Technologies). For simulation of contrast administration in the CTA protocols, bolus-tracking sequences (SureStart Protocol, Toshiba Medical Systems) were performed. Bolus-tracking sequences were performed to determine the arrival of the contrast medium bolus in the target area and to start the scanning at the time of optimal contrast enhancement. A SureStart time of 14 seconds was used on both scanners, during which continuous scans were acquired at the selected level to simulate manual bolus tracking. A 14-second SureStart time corresponds to a very long circulation time in patients. In the actual clinical situation, SureStart sequences are acquired with a delay of 10 seconds after contrast injection because no contrast medium is expected to arrive in the target vessels before that time. No test bolus simulation was performed for the combo protocol or CTP imaging.

Table 3: Parameters of the protocols used on the 64-row CT scanner

	Noncontrast Head CT Scan			
Parameter	Infratentorial	Supratentorial	CTP	CTA
Lens protection	No		Yes	Yes
Collimation (mm)	2 × 4		4 × 8	0.5 × 64
Table increment (mm)	8 mm	8 mm	None	20.5
Pitch	1		No	0,614
Tube current (mAs_{eff})	375	250	50	150
Tube current (mA)	250		50	300
Voltage (kV)	120		120[a]	120
Rotation time	1.5 s	1.0 s	1 s	0.5 s
Scan length (mm)	140		32	340.8
Total scan time	24.8 s		45.7 s	23 s
Gantry angulation	Yes		Yes	No

[a] The Aquilion 64 scanner at the Department of Radiology, Charité Campus Mitte (Berlin, Germany) was one of the first scanners of this type installed. Due to a technical limitation, this Aquilion 64 scanner does not support CTP with 80 kV. Newer versions of the Aquilion 64 scanner allow performing CTP with 80 kV in the same way as the Aquilion ONE does.

Calculation of Effective Dose

The effective dose is defined as the sum of the organ-equivalent doses weighted by the ICRP 103 organ-weighting factors. Not all organ doses listed for the remaining body regions in the ICRP 103 guideline were taken into account in this calculation. These body regions have a very small weighting factor (0.0086) and are far away from the scanning area (except for the thymus and oral mucosa); therefore, we assumed that their contribution to the effective dose would be negligible. For organs only partially in the scanning area (skin, bone marrow [spinal column]), a mean total organ dose was calculated from the mean values measured within and outside the scanning area. Effective doses were calculated separately for men and women.

Results

Organ Doses. The highest organ dose measured in the neurocranium was 92.0 mGy (combo protocol skin dose in the scanning area on the 320-detector row scanner). The maximum mean thyroid organ dose was measured for the sequences that contain SureStart scans (helical CTA in 64-detector row CT and helical neck CTA in 320-detector row CT) and was 58.6 mGy on the 320-detector row CT scanner and 39.17 mGy on the 64-detector row scanner (CTA). The maximum doses to organs in the head differ between the 2 perfusion protocols (CTP on the 64-detector row scanner and combo on the 320-detector row scanner) because the scanning area is smaller for 64-detector row CTP. The eye lenses and pituitary gland are outside the scanning area for 64-detector row CTP.

The low doses determined for 320-detector row CTA in neurocranial organs compared with 64-detector row CT (mean maximum values determined by skin dosimeters of 3.8 versus 26.3 mGy) can be attributed to the 320-detector row CTA protocol being restricted to the neck vessels (scanning area from T5 to the skull base versus T5 to the vertex for 64-detector row CTA), while the cerebral vessels are scanned as part of the combo protocol. The measured genital doses ranged from 0.3 mGy (ovaries, noncontrast head CT on the 64-detector row CT scanner) to 1.0 mGy (ovaries, noncontrast incremental head CT on the 320-detector row CT scanner).

Eye Lens Dose. Incremental CCT without eye lens protection resulted in mean eye lens doses of 41.7 mGy (64-detector row CT) and 44.3 mGy (320-detector row CT). The doses determined for the same protocols with eye lens protection were the following: 6.7 mGy (CTP, 64-detector row CT), 14.9 mGy (CTA, 64-detector row CT), 44.0 mGy (combo, 320-detector row CT), and 2.4 mGy (neck CTA, 320-detector row CT). To verify this result and to exclude potential bias resulting from the use of different eye lens protectors, we additionally measured the lens dose of the volume CTP protocol by using the calibrated film verification method (CTDI phantom and measurement films) without and with both lens-protection shields investigated (same manufacturer and type). This second measurement yielded a surface dose for the eyes (comparable with the eye lens dose) for the combo protocol for whole-brain perfusion by using the 320-detector row CT scanner of 140 mGy without and 65 mGy with lens protection, corresponding to a 54% lens dose reduction for this protocol. There were no differences between the 2 lens-protection devices used. The markedly higher skin doses measured by using the film method can be explained by the fact that the distance between the surface detectors and the radiation source is shorter when the CTDI phantom is used because the Alderson-Rando phantom has a smaller skull diameter.

Comparison of the doses measured in different body regions and organs (Table 1) shows that the organ doses in the head (hemispheres and pituitary glands) are smaller for the 320-detector row volume scan than for incremental CCT on the same scanner, while the overall dose distribution is similar for both protocols.

Effective Dose. The effective dose for complete stroke imaging was calculated by adding the measured organ doses multiplied by weighting factor (ICRP 103). The calculated effective dose resulted in 7.52/7.54 mSv (m/f) for 64-detector row CT and 10.56/10.6 mSv (m/f) for 320-detector row CT. The dose differences are due to the approximately 4 times larger z-coverage of the 320-detector row CT (14 cm in the protocol investigated here) compared with 64-detector row CT (3.2 cm).

Discussion

To our knowledge, this study is the first to investigate the radiation dose of stroke imaging on the new 320-detector row CT scanner in comparison with conventional 64-detector row CT scanners. Our results show the radiation dose of complete stroke imaging to be higher on the new scanner. However, one has to keep in mind that z-axis coverage for whole-brain perfusion imaging is clearly larger. Moreover, the protocols used on the 2 CT scanners are not fully comparable. The 2 most important differences are the following: 1) the scanning areas of the perfusion protocols are different (ie, whole-brain coverage in 320-detector row CTP versus 3.2-cm fractional brain coverage in 64-detector row CTP), and 2) the intracranial part of the cerebral CTA is performed as a dynamic study in 320-detector row CTA. An analysis of both CTA protocols in terms of image quality for evaluation of vessel caliber, small arteries, and aneurysms has been performed in another study.[16]

Initial results have also been reported by Klingebiel et al.[17] Tube potential also is an important factor for improvement of radiation dose and image quality. The use of a lower tube potential on the 320-detector row CT scanner is also supported by other investigators who see this as an option to reduce the radiation dose while at the same time increasing the contrast-to-noise ratio of CTA and CTP.[18] The 64-detector

Table 4: Parameters of the protocols used on the 320-row CT scanner

Parameter	Noncontrast Head CT Scan (Volume)	Noncontrast Head CT (Incremental)		Combo (Cerebral CTA + CTP)	Neck CTA
		Infratentorial	Supratentorial		
Lens protection	No	No	Yes	Yes	
Collimation (mm)	0.5 × 280	2 × 4	2 × 4	0.5 × 320	0.5 × 64
Table increment (mm)	No	8	8	none	20.5
Pitch		1	1	no	0.614
Tube current (mAs_{eff})	320	375	250	100	Tube current modulation
Tube current (mA)	320	250		100	Tube current modulation
Voltage (kV)	120	120		80	120
Rotation time	1 s	1.5 s	1 s	1 s	0.5 s
Scan length (mm)	140	140		160	216
Scan time	7.2 s	26.8 s		29.8 s	30.99 s
Gantry angulation	Yes	Yes	Yes	No	No

row CT scanner we used in our study was a first-generation Aquilion 64 (Toshiba Medical Systems) and did not support perfusion imaging at 80 kV, which is possible on newer generation scanners of this type and also on the Aquilion ONE (Toshiba Medical Systems). According to the $CTDI_v$ data due to the read out from a CT scan console, the use of perfusion imaging at 80 kV could result in an approximately 73.8% reduction of the dose when using the same protocol. In our phantom measurements, we used the standard protocols optimized for comprehensive stroke imaging on each scanner.

A possible advantage of fast scanning during a single rotation is the reduction of motion artifacts compared with incremental CCT. On the other hand, if motion occurs during a single-rotation scan, the resulting artifacts affect all sections. Studies concerning the value of volume scanning compared with incremental scanning in terms of image quality are not yet available, to our knowledge. The radiation dose for volume scanning is comparable with the radiation dose of incremental CCT in a 64-detector row CT scanner (effective dose in men: volume scan, 1.62 mSv; 64-detector row incremental CCT, 1.65 mSv).

Concerning measured organ doses of the thyroid, the discrepancy between the 2 scanners cannot be explained by the protocols used alone; it may be due to a measurement error. The experimental setup used in our study overestimated the thyroid dose. A SureStart scanning time of 14 seconds corresponds to a very long circulation time. The high thyroid dose resulting from manual bolus tracking in the neck area by using the SureStart technique underlines the importance of protocol design and the search for alternatives to reduce excessive radiation exposure. The thyroid dose is lower in the routine clinical setting because scans for bolus tracking are acquired with a delay of 10 seconds.

Another option to reduce the radiation dose is to use discontinuous scanning. Instead of the SureStart option, the scanning delay can be determined by test bolus administration for calculating the arrival time and scanning delay for the subsequent diagnostic scan. A study of coronary artery CT has shown enhancement to be more homogeneous when bolus tracking is used compared with the test bolus method.[15] We, therefore, use bolus tracking for CT scanning of head and neck vessels in routine clinical examinations. Test bolus administration is used for perfusion imaging: The scan for determining arrival of the test bolus is positioned intracranially, precluding relevant exposure of the most radiation-sensitive head and neck organs. When one performs CT perfusion in the setting of stroke imaging, it is recommended to determine the delay for CTA of the neck vessels from test bolus administration instead of acquiring an additional SureStart sequence. This will significantly reduce the thyroid organ dose.

The discrepancy between the measured genital doses for both scanners may be due to the fact that in this region only scattered radiation is measured and TLDs are not exact for the measurement of low doses.

As with all dose measurements, the doses determined in our study are dependent on the protocols used. The protocols we used in this experimental investigation were implemented and optimized in cooperation with the manufacturer in the setting of feasibility studies. Their practicality is also ensured because they have run smoothly and successfully under routine clinical conditions for >1 year.[17] Our experience with these protocols suggests that they are suitable for stroke imaging in terms of image quality. Because we do not use other protocols like a toggling technique in our institution, those were not included in this study. Expanding the study to include other stroke protocols, such as the toggling technique, could provide another important data point for dose considerations. Because the protocols we used here have been optimized for the intended purpose, dose reduction efforts should not aim at changing these protocols but rather at selecting the most suitable method for determining circulation time and using new techniques such as volume imaging instead of incremental CCT.

Comparison of our Results with Published Organ Doses. Table 3 lists all organ doses of the entire stroke protocol investigated in our study. The doses determined with the parameters used on the 64-detector row CT scanner are slightly above the values reported in the literature[19]; however, the reported doses were obtained for multisection CT scanners from different manufacturers with different z-coverages and the use of different tube potentials (kilovolts) for perfusion imaging. No data are available for comparison with the doses we measured for the 320-detector row CT protocol.

The lens dose for volume perfusion imaging on the 320-detector row CT scanner is higher than the dose for perfusion imaging on the 64-detector row scanner. Several factors contribute to this difference: The eyes are not within the scanning area in 64-detector row CT, z-coverage is much larger for the

320-detector row CT protocol (14 versus 3.2 cm), and the volume scan simultaneously provides the data for CTA. For a true comparison, one would have to add the doses for the CTA protocol on the 64-detector row CT scanner. Nevertheless, the lens dose is clearly highest for the volume CTP protocol even when lens protection is used. The dose-reducing effect of the lens protection shield is clearly evident for CTA and the combo protocol and comparable with that in the literature.[20-23] With standard settings without gantry angulation, the eye lenses are within the scanning area. We used no lens protection for the incremental scans. Lens protection is not absolutely necessary because the lenses are outside the beam when a standard scanning area with angulation at the supraorbitomeatal line is used. In our department, we use lens protection for all routine head CTs. The metallic fixation of the phantom precluded optimal gantry angulation, which is why the lenses were within the scanning area in our experimental setup.

Conclusions

The new 320-detector row CT scanner generation enables perfusion imaging of the entire neurocranium and dynamic CTA of the intracranial vessels. Our experimental results suggest that perfusion imaging on the new CT scanner is associated with a higher effective dose while z-coverage is also larger. Here, the physician has to weigh the expected diagnostic benefits against the risks of a higher radiation dose. Further studies are needed to evaluate the advantages of the new imaging options and to define those diagnostic questions that will justify the higher radiation exposure as opposed to cases in which a multisection CT scan with a smaller z-coverage field may be preferred.

References

1. Bohner G, Förschler A, Hamm B, et al. **Quantitative perfusion imaging by multi-slice CT in stroke patients** [in German]. *Rofo* 2003;1785:806–13
2. Hoeffner E, Case I, Jain R, et al. **Cerebral perfusion CT: technique and clinical applications.** *Radiology* 2004;231:632–44. Epub 2004 Apr 29
3. Roberts HC, Roberts TP, Smith WS, et al. **Multisection dynamic CT perfusion for acute cerebral ischemia: the "toggling-table" technique.** *AJNR Am J Neuroradiol* 2001;22:1077–80
4. Boone JM. **The trouble with CTDI 100.** *Med Phys* 2007;34:1364–71
5. Kyriakou Y, Deak P, Langner O, et al. **Concepts for dose determination in flat-detector CT.** *Phys Med Biol* 2008;53:3551–66. Epub 2008 Jun 13
6. Geleijns J, Salvadó Artells M, de Bruin PW, et al. **Computed tomography dose assessment for a 160 mm wide, 320 detector row, cone beam CT scanner.** *Phys Med Biol* 2009;54:3141–59. Epub 2009 May 6
7. Mori S, Endo M, Nishizawa K, et al. **Comparison of patient doses in 256-slice CT and 16-slice CT scanners.** *Br J Radiol* 2006;79:56–61
8. Mori S, Endo M, Nishizawa K, et al. **Enlarged longitudinal dose profiles in cone-beam CT and the need for modified dosimetry.** *Med Phys* 2005;32:1061–69
9. Mori S, K. Nishizawa, Ohno M, et al. **Conversion factor for CT dosimetry to assess patient dose using a 256-slice CT scanner.** *Br J Radiol* 2006;79:888–92. Epub 2006 May 25
10. **The 2007 Recommendations of the International Commission on Radiological Protection: ICRP publication 103.** Ann ICRP 2007;37:1–332
11. Dixon RL, Ekstrand KE. **A film dosimetry system for use in computed tomography.** *Radiology* 1978;127:255–58
12. Shope TB, Morgan TJ, Showalter CK, et al. **Radiation dosimetry survey of computed tomography systems from ten manufacturers.** *Br J Radiol* 1982;55:60–69
13. Zink FE, McCollough CH. **The measurement of radiation dose profiles for electron beam computed tomography using film dosimetry.** *Med Phys* 1994;21:1287–91
14. McCollough CH, Zink FE, Morn RL. **Radiation dosimetry for electron beam CT.** *Radiology* 1994;192:637–43
15. Cademartiri F, van der Lugt A, Luccichenti G, et al. **Parameters affecting bolus geometry in CTA: a review.** *J Comput Assist Tomogr* 2002;26:598–607
16. Siebert E, Bohner G, Dewey M, et al. **320-slice CT neuroimaging: initial clinical experience and image quality evaluation.** *Br J Radiol* 2009;82:561–70
17. Klingebiel R, Siebert E, Diekmann S, et al. **4-D imaging in cerebrovascular disorders by using 320-slice CT: feasibility and preliminary clinical experience.** *Acad Radiol* 2009;16:123–29
18. Bahner ML, A. Bengel, Brix G, et al. **Improved vascular opacification in cerebral computed tomography angiography with 80 kVp.** *Invest Radiol* 2005;40:229–34
19. Cohnen M, Wittsack HJ, Assadi S, et al. **Radiation exposure of patients in comprehensive computed tomography of the head in acute stroke.** *AJNR Am J Neuroradiol* 2006;27:1741–5
20. Colombo P, Pedroli G, Nicoloso M, et al. **Evaluation of the efficacy of a bismuth shield during CT examinations.** *Radiol Med* 2004;108:560–68
21. Hein E, Rogalla P, Klingebiel R, et al. **Low-dose CT of the paranasal sinuses with eye lens protection: effect on image quality and radiation dose.** *Eur Radiol* 2002;12:1693–96. Epub 2002 Feb 2
22. Keil B, Wulff J, Schmitt R, et al. **Protection of eye lens in computed tomography: dose evaluation on an anthropomorphic phantom using thermo-luminescent dosimeters and Monte-Carlo simulations** [in German]. *Rofo* 2008;180:1047–53. Epub 2008 Nov 28
23. Hopper KD, Neuman JD, King SH, et al. **Radioprotection to the eye during CT scanning.** *AJNR Am J Neuroradiol* 2001;22:1194–98